ACCOUNTS
of chemical research

Proton-Detected Solid-State NMR Spectroscopy at Aliphatic Sites: Application to Crystalline Systems

SAM ASAMI[§] AND BERND REIF*[,§,‡]

[§]*Deutsches Forschungszentrum für Gesundheit und Umwelt (HMGU), Helmholtz-Zentrum München, Ingolstädter Landstr. 1, D-85764 Neuherberg, Germany, and* [‡]*Munich Center for Integrated Protein Science (CIPSM) at Department of Chemie, Technische Universität München (TUM), Lichtenbergstr. 4, D-85747 Garching, Germany*

RECEIVED ON MARCH 14, 2013

CONSPECTUS

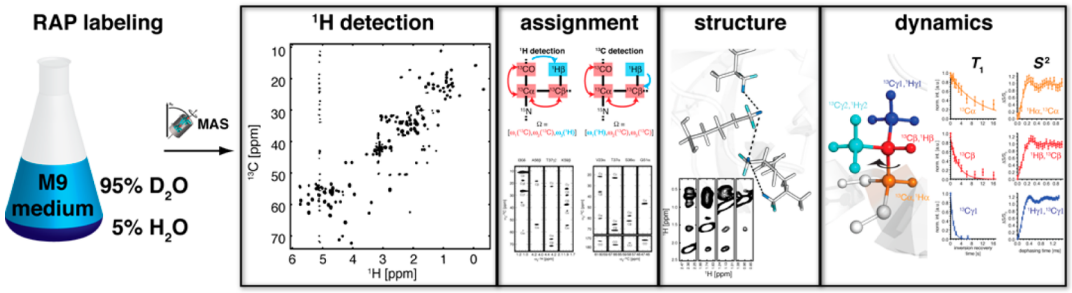

When applied to biomolecules, solid-state NMR suffers from low sensitivity and resolution. The major obstacle to applying proton detection in the solid state is the proton dipolar network, and deuteration can help avoid this problem. In the past, researchers had primarily focused on the investigation of exchangeable protons in these systems.

In this Account, we review NMR spectroscopic strategies that allow researchers to observe aliphatic non-exchangeable proton resonances in proteins with high sensitivity and resolution. Our labeling scheme is based on u-[^{2}H,^{13}C]-glucose and 5−25% H_2O (95−75% D_2O) in the M9 bacterial growth medium, known as RAP (reduced adjoining protonation). We highlight spectroscopic approaches for obtaining resonance assignments, a prerequisite for any study of structure and dynamics of a protein by NMR spectroscopy. Because of the dilution of the proton spin system in the solid state, solution-state NMR ^{1}HCC^{1}H type strategies cannot easily be transferred to these experiments. Instead, we needed to pursue (^{1}H)CC^{1}H, CC^{1}H, ^{1}HCC or (^{2}H)CC^{1}H type experiments. In protonated samples, we obtained distance restraints for structure calculations from samples grown in bacteria in media containing [1,3]-^{13}C-glycerol, [2]-^{13}C-glycerol, or selectively enriched glucose to dilute the ^{13}C spin system. In RAP-labeled samples, we obtained a similar dilution effect by randomly introducing protons into an otherwise deuterated matrix. This isotopic labeling scheme allows us to measure the long-range contacts among aliphatic protons, which can then serve as restraints for the three-dimensional structure calculation of a protein. Due to the high gyromagnetic ratio of protons, longer range contacts are more easily accessible for these nuclei than for carbon nuclei in homologous experiments.

Finally, the RAP labeling scheme allows access to dynamic parameters, such as longitudinal relaxation times T_1, and order parameters S^2 for backbone and side chain carbon resonances. We expect that these measurements will open up new opportunities to obtain a more detailed description of protein backbone and side chain dynamics.

Introduction

In the solid-state, generally heteronuclei are detected as strong dipole−dipole interactions often prevent the sensitive detection of individual protons. Due to its high gyromagnetic ratio, the proton, however, is the ideal nucleus for detection and correlation spectroscopy. Three strategies in principle allow to tackle the line width problem: fast spinning, homonuclear decoupling, and dilution of the proton spin bath. Ultrafast MAS (60−70 kHz) has been pushed forward by Samoson and co-workers[1] and has been applied recently successfully to uniformly protonated samples by Rienstra, Pintacuda, and Emsley.[2,3] ^{1}H,^{1}H homonuclear decoupling approaches did not succeed in reducing the unscaled proton line widths to values below 150−300 Hz

Published on the Web 06/07/2013 www.pubs.acs.org/accounts
10.1021/ar400063y

(i.e., 0.25−0.5 ppm at 600 MHz).[4,5] Deuteration chemically eliminates proton dipolar interactions. In the solid-state, deuteration was first applied to small molecules[6−8] and then later extended to peptides[9−11] and proteins.[4,12−14] Thereby, nonexchangeable sites are deuterated in the first place. The amount of H_2O/D_2O in the crystallization buffer allows adjustment of the proton concentration at exchangeable sites to yield sufficiently reduced proton dipolar couplings at a given MAS rotation frequency.[15−17] The labeling scheme could successfully be applied to amyloid fibrils,[18−20] membrane proteins,[18,20,21] and protein−RNA complexes.[22] The spectral quality of the above-mentioned examples appears to be lower in comparison to microcrystalline protein preparations. We expect, however, that resolution will increase with improved sample preparations. In fact, bacteriorhodopsin yields the most narrow resonances, indicating that sample homogeneity is an important factor.

Deuteration schemes, which rely on amide back-exchange, are difficult to implement for proteins, which have very stable amide protons that do not exchange within months. Samples can only be efficiently prepared when H/D exchange can be catalyzed, for example, by unfolding and refolding of the protein, such that labile protons can be substituted with deuterons from the medium. Refolding to the native state can be difficult, for example, for membrane proteins that need to be functionally reconstituted in the lipid bilayer. H/D exchange can be avoided by employing specific precursors of amino acid biosynthesis, which yield specifically ILV methyl labeled samples.[23−25] However, this scheme has the disadvantage that not all aliphatic sites are accessible. Furthermore, methyl groups in the hydrophobic core of a protein often cluster, which induces an increased line width due to dipole mediated line broadening.

We recently presented a labeling scheme, which does not require an H/D exchange step and retains at the same time the spectroscopic benefits of high-resolution ^{1}H-detection. In order to reduce the proton density of nonexchangeable protons in a protein, we employ a M9 bacterial growth medium that contains u-[^{2}H,^{13}C]-glucose and 5−25% H_2O (95−75% D_2O). The approach is coined RAP (reduced adjoining protonation).[26] Figure 1 shows a ^{1}H-detected ^{1}H,^{13}C HMQC spectrum of a microcrystalline α-spectrin SH3 5% RAP sample. Already at a moderate MAS frequency of 20 kHz and an external magnetic field of 14.1 T (600 MHz), high resolution is obtained for the entire aliphatic region.

The experimental proton line widths in Figure 1 vary between 25 Hz for Thr37γ2 and 60 Hz for Thr37α. The RAP labeling scheme allows avoidance of high-power decoupling.

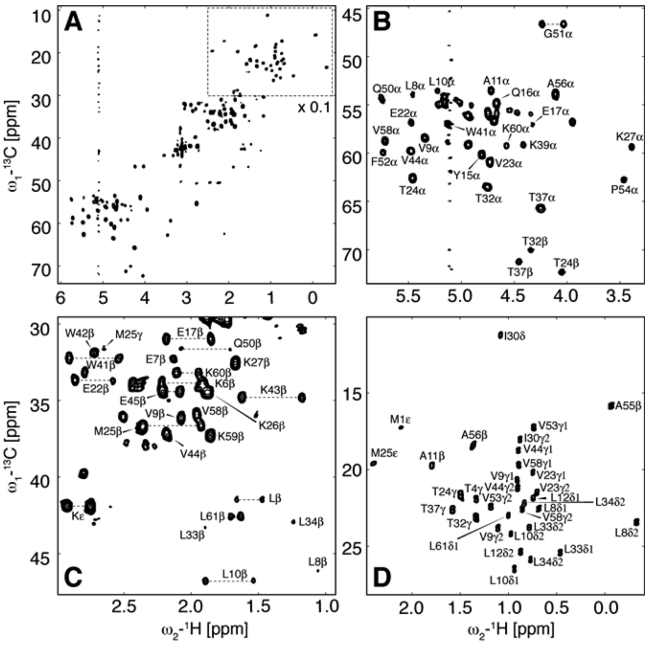

FIGURE 1. MAS solid-state ^{1}H-detected ^{1}H,^{13}C HMQC spectrum of the SH3 domain of α-spectrin.[26] The sample was produced by growing bacteria in a M9 minimal medium that contains 5% H_2O and 95% D_2O. The spectrum was recorded at 600 MHz (14.1 T). The full spectrum (A) is represented enlarged in panels B, C, and D displaying the ^{1}Hα/^{13}Cα, ^{1}Hβ/^{13}Cβ, and the methyl regions, respectively. The intensities for resonances of the methyl region in panel A have been scaled by a factor of 0.1. Reproduced with permission from ref 26. Copyright 2010 American Chemical Society.

A rf field of 2−3 kHz is sufficient to achieve ^{13}C decoupling using WALTZ-16 during ^{1}H-detection.[27] In comparison to experiments in which the residual protonation of a sample is exploited (originating from the proton impurities of the utilized 97% isotopically enriched deuterated glucose and 99% D_2O medium), the sensitivity is significantly enhanced.[28]

The Optimal RAP Sample

The ideal proton concentration in the M9 growth medium depends on the MAS rotation frequency, which will be employed later on in the NMR investigation. On one hand, more protons can potentially increase the achievable sensitivity. On the other hand, proton−proton dipolar interactions will induce a broadening of the resonances. In addition, isotope induced chemical shift changes and the presence of the isotopomers $^{13}CD_2H$, $^{13}CDH_2$, and $^{13}CH_3$ might broaden the carbon resonances, when too high concentrations of H_2O are employed. For a 5% RAP sample, we find, that the methyl and backbone proton signal intensities reach a plateau value at around 40 kHz, employing a ^{1}H,^{13}C HMQC sequence (Figure 2A).[29] For a 25% RAP sample, this plateau is reached at MAS rotation frequencies of around 60 kHz, indicating, that this rotation frequency is sufficient to achieve

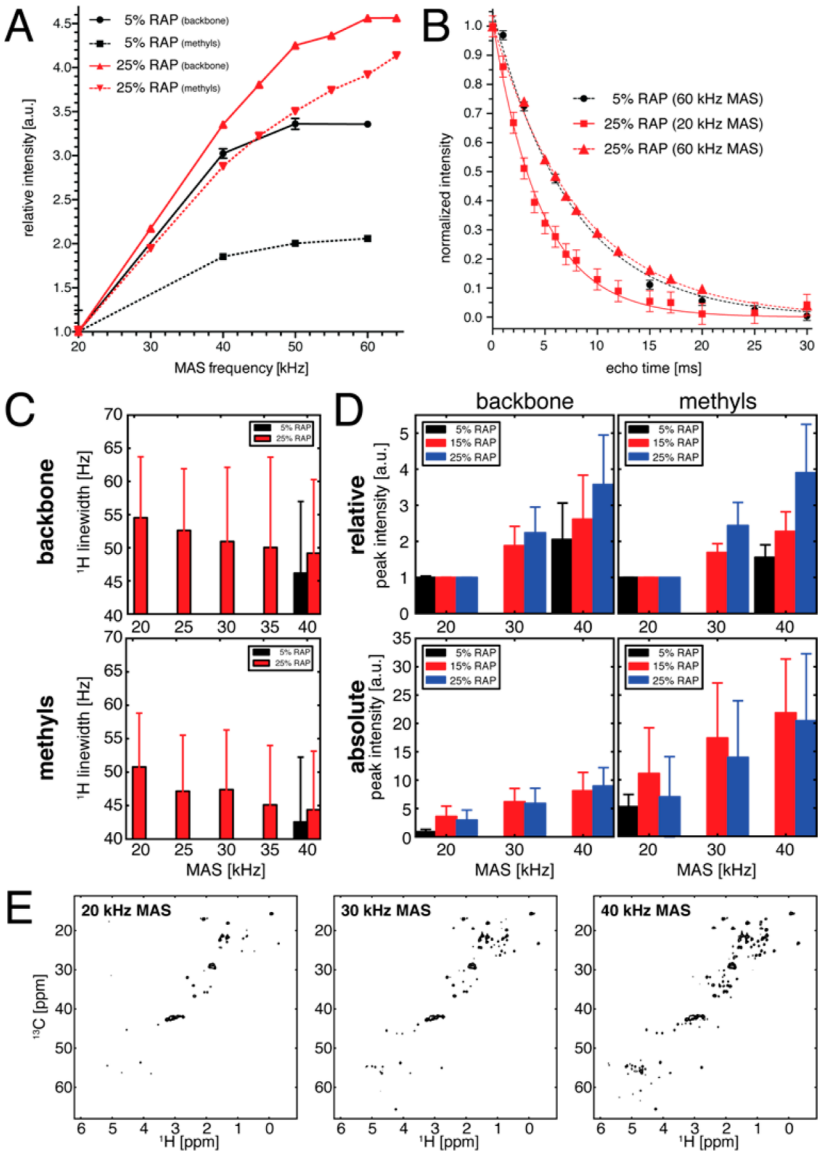

FIGURE 2. (A) Integral intensity for backbone and methyl resonances for the first FID from a $^{1}H,^{13}C$ HMQC experiment as a function of the MAS frequency for SH3 RAP samples grown on M9 medium containing either 5% or 25% H_2O, respectively.[29] The signal intensity reaches a plateau at a MAS frequency of ~40 (~60) kHz for the 5% (25%) RAP sample. The sensitivity gain amounts to a factor of ~3.5 (~4.5) and ~2.0 (~4.0) for backbone and methyl resonances. (B) ^{1}H signal dephasing in a T_2 echo experiment at 20 and 60 kHz. The T_2 time for the 25% RAP sample increases from 4.6 to 8.2 ms at higher spinning frequencies and becomes comparable to the bulk T_2 of the 5% RAP sample (7.5 ms). (C) Average methyl and backbone ^{1}H line width as a function of the MAS frequency for a 5% and 25% RAP sample of α-spectrin SH3. (D) Relative and absolute signal intensities as a function of the MAS rotation frequency for a 5%, 15%, and 25% SH3 RAP sample. The intensities were extracted for individual resolved resonances from 2D $^{1}H,^{13}C$ HMQC spectra. (E) 2D $^{1}H,^{13}C$ HMQC spectra for a 25% RAP sample at different MAS rotation frequencies. A significant increase in sensitivity for both backbone and side chain resonances is observed. All spectra are plotted using the same contour levels with respect to the noise rmsd. Experimental parameters are kept the same in all experiments, except for the MAS rotation frequency. Reproduced with permission from ref 29. Copyright 2012 Springer.

an efficient averaging of proton−proton dipolar interactions. This is also reflected in the echo ^{1}H T_2 times, which become equal for the 5% and 25% RAP sample at a MAS rotation frequency of 60 kHz (Figure 2B). At fast spinning (40 kHz), the average proton resonance line widths of the 25% RAP samples reach the limiting line width values of the 5% RAP sample (Figure 2C). As the proton concentration is increased for the 15% and 25% RAP samples, the relative and absolute intensities of the correlation peaks are increased accordingly (Figure 2D,E).

^{1}H- and ^{13}C-Detected Aliphatic Backbone and Side Chain Assignment Experiments

Assignments are essential to proceed with investigations of structure and dynamics. In RAP samples, assignments are more difficult to obtain in comparison to homogeneously

labeled samples, due to the stochastic incorporation of protons. For that reason, HCCH type experiments cannot easily be implemented. For RAP samples, complementary assignment strategies need to be established. We found that all resonances can be unambiguously assigned using 3D HCC and CCH type correlation experiments, yielding assignment of ~90% of the ^{1}Hα,^{13}Cα backbone and side chain resonances of a 15% RAP sample of α-spectrin SH3.[30] In both experiments, carbon−carbon mixing is achieved using an adiabatic RFDR sequence.[31] Active recoupling of the ^{13}C,^{13}C dipolar interactions is essential in deuterated samples, because the transfer amplitudes in proton driven spin diffusion (PDSD) experiments is typically not sufficient to yield efficient mixing.

In Figure 3, the performance of the dipolar mixing sequences PDSD,[32] adiabatic RFDR,[31] and RAD/DARR[33,34] are compared, employing a uniformly protonated as well as a 5% RAP sample of α-spectrin SH3. We find similar mixing performance for a 5% RAP labeled sample (B, adiabatic RFDR spectrum using a mixing time of 15 ms) in comparison to the uniformly protonated SH3 sample (A, PDSD spectrum using a mixing time of 20 ms). Application of PDSD mixing to a severely proton diluted 5% RAP sample yielded a very limited number of cross peaks (C), even though the mixing time was increased to 50 ms. Under these conditions, RAD/DARR spectra displayed a significantly improved mixing profile.[35] In the experiment, a rf field is applied either on the ^{1}H channel (D), on the ^{2}H channel (E), or, as recently proposed,[36] simultaneously on the ^{1}H and the ^{2}H channels (F). Simultaneous irradiation only yielded marginal improvements over single-channel irradiation. For the cross peak Thr32 ^{13}Cβ−^{13}Cα, we find a relative cross peak intensity of 47% for RFDR and 15% for ^{1}H+^{2}H RAD/DARR (the percentage indicates the ratio of the cross peak volume to the sum of the cross and diagonal peak volumes). In total, the adiabatic RFDR sequence (subjacent spectrum in black in plots C−F) displayed by far the best mixing profile among PDSD and RAD/DARR and was, therefore, employed in 3D HCC and CCH assignment experiments.[30]

The 3D CCH experiment exploits ^{13}C PREs to accelerate data acquisition and proton detection for high sensitivity.[37,38] In order to improve the resolution, the spectral width was reduced to the aliphatic region. Therefore, the CP condition was optimized to suppress ^{13}CO excitation and prevent folding artifacts (Figure 3G). Originally, the 3D CCH experiment was recorded with carbon direct excitation. Alternatively, the experiment can be performed by transferring magnetization simultaneously from the deuteron and the proton to the carbon spin.[30,39] The 3D HCC experiment allows easy assignment of ^{1}Hα resonances in cases where the ^{1}Hα resonance is perturbed by the solvent signal. Homonuclear scalar decoupling in the indirect and direct carbon dimension

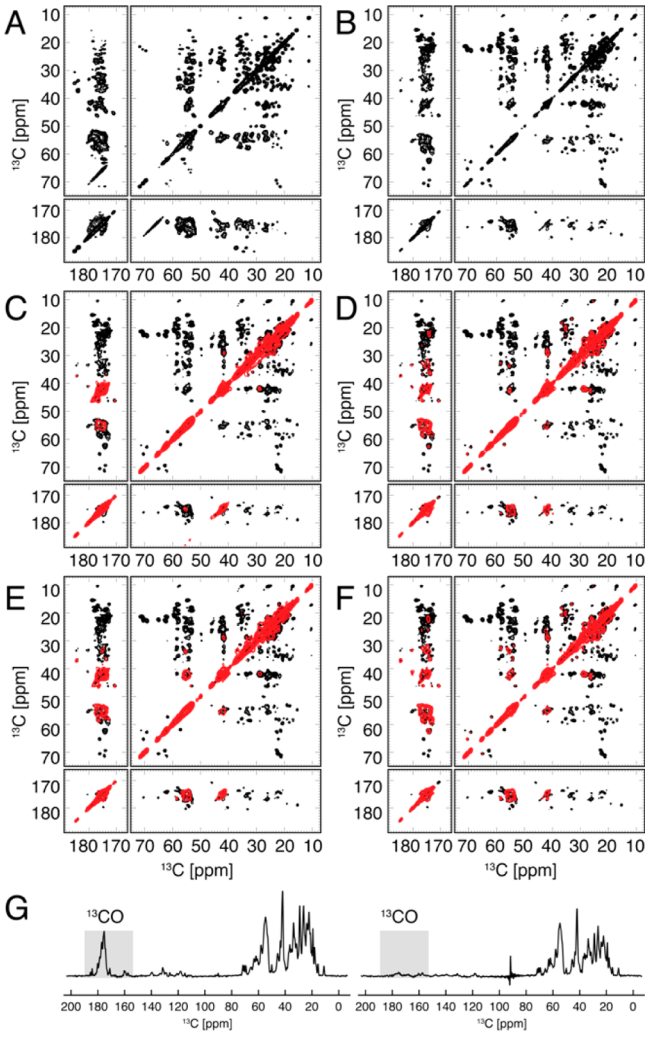

FIGURE 3. (A) PDSD spectrum of a uniformly [^{1}H,^{13}C,^{15}N]-labeled α-spectrin SH3 sample recorded at 400 MHz and 11 kHz MAS. The mixing time was set to 20 ms. (B) Adiabatic RFDR[31] spectrum acquired for a 5% RAP sample at 600 MHz and 20 kHz MAS. The mixing period was adjusted to 15 ms. This spectrum was used as a reference for panels C−F. The superimposed red spectra in panels C−F are PDSD and RAD/DARR spectra with rf irradiation on the ^{1}H, ^{2}H, and ^{1}H+^{2}H channel. All spectra C−F were recorded using a total mixing time of 50 ms and a 5% SH3 RAP sample. The rf field strength was set to the $n = 1$ rotary resonance condition. (G) Optimization of selective excitation during the ^{1}H,^{13}C CP magnetization transfer for a 25% RAP sample. $^{1}H^{N}$ amide protons were back-exchanged in a 30%/70% H_2O/D_2O buffer. The ^{13}C offset was set to the middle of the aliphatic region and the CP contact time to 1 ms. The spectra were recorded at a MAS frequency of 20 kHz and an external magnetic field of 16.4 T (700 MHz). Either a (left) linear ramp from 100% to 75% or (right) no ramp was employed. Omitting the ramp during CP and optimizing for maximum sensitivity for aliphatic resonances reduced the CO signals (gray shaded area) by almost a factor of 10.

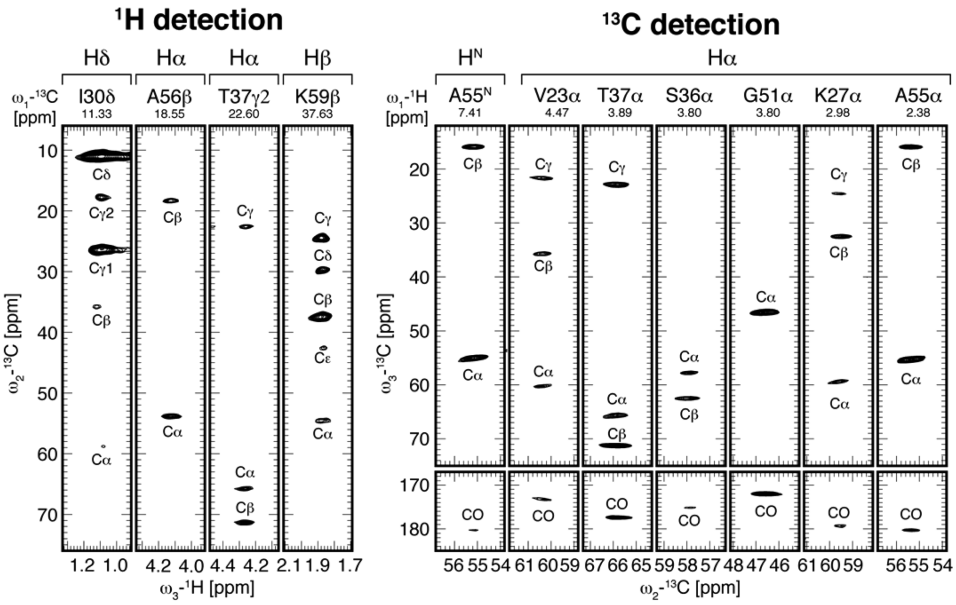

FIGURE 4. Two-dimensional strips extracted from the 3D ^{1}H-detected CCH (left) and the ^{13}C-detected HCC correlation experiment (right) recorded for a 15% RAP sample of the α-spectrin SH3 domain.[30] $^{1}H^{N}$ as well as ^{1}Hα chemical shifts can be unambiguously assigned by correlating ^{13}Cα to $^{13}C\beta/^{13}$CO chemical shifts. Reproduced with permission from ref 30. Copyright 2012 Springer.

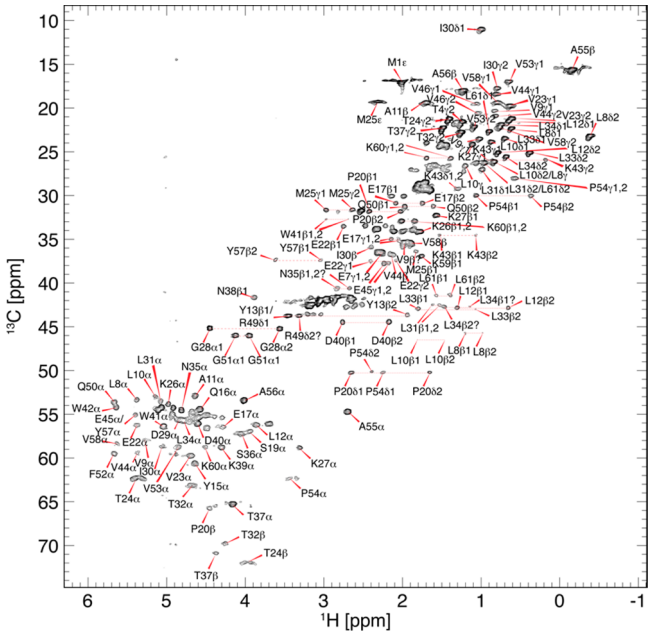

FIGURE 5. Assigned ^{1}H,^{13}C correlation spectrum of a 25% RAP sample of α-spectrin SH3. The spectrum was recorded at a magnetic field strength of 20.0 T (850 MHz) and a MAS rotation frequency of 40 kHz.

allows significant increase in spectral resolution.[30,40] Representative strip plots of the 3D HCC and the 3D CCH experiment are shown in Figure 4. In particular for sequential assignment experiments, a four-channel probe with high-power capabilities for ^{1}H, ^{2}H, ^{13}C, and ^{15}N in combination with optimum control strategies to overcome bandwidth limitations will yield a further increase in experimental sensitivity.[41]

The assigned ^{1}H,^{13}C correlation spectrum is represented in Figure 5. The spectrally achievable resolution is obviously very high and should pave the way for a detailed analysis of structure and dynamics.

Determination of the Protein Tertiary Structure

Aliphatic protons are most essential for the determination of tertiary structure restraints. For structure calculation in the solid-state, routinely, ^{13}C,^{13}C distance restraints,[42] as well as dihedral restraints, are employed.[43] The precision of the calculated tertiary protein structure benefits in particular from long-range restraints involving side chains. Due to their peripheral localization, protons are ideally suited to deliver nontrivial distance restraints. ^{1}H,^{1}H distance restraints can be obtained in XHHY (X, Y = C or N) type experiments.[12,44,45] These experiments suffer, however, from a low signal-to-noise level due to the detection of low-γ nuclei.

In uniformly labeled samples, long-range interactions are difficult to obtain due to the truncation of the dipolar coupling. Therefore, labeling schemes are exploited that rely on spin dilution.[42] In RAP samples, the proton spin system was diluted to enable high-resolution proton detection.[26]

In the experiment, a first proton evolution period is followed by a ^{1}H,^{1}H magnetization mixing step, utilizing a rotor synchronized adiabatic RFDR mixing scheme (Figure 6A).[31] After mixing, magnetization is transferred to ^{13}C for chemical shift evolution and finally to ^{1}H for detection, using a scalar

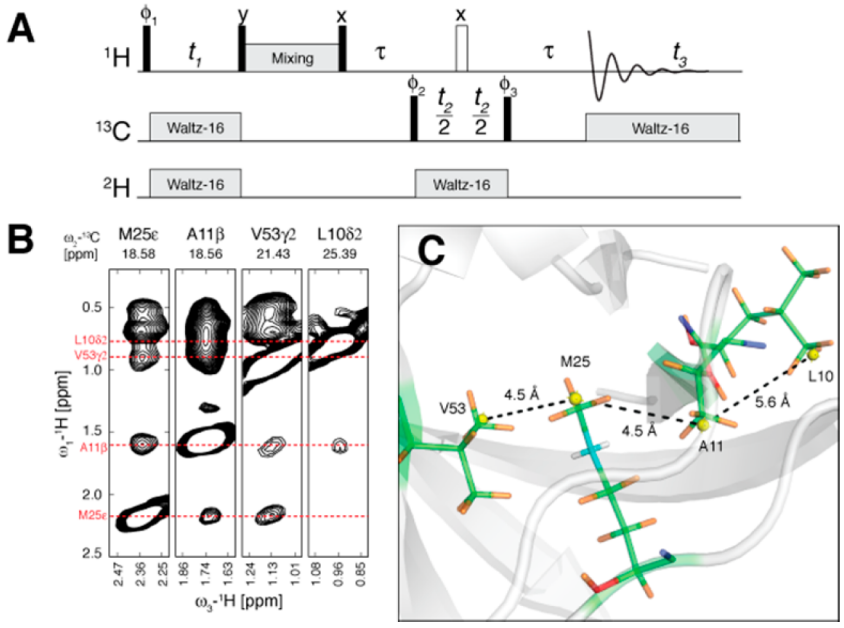

FIGURE 6. Three-dimensional H(H)CH correlation experiment for the determination of long-range ^{1}H,^{1}H distances in the solid-state. (A) The pulse sequence is based on a solution-state ^{1}H,^{13}C NOESY–HMQC experiment. For ^{1}H,^{1}H mixing, a rotor synchronized adiabatic RFDR mixing scheme was used.[31] (B) Two-dimensional strips along the ω_2-^{13}C dimension of M25ε, A11β, V53γ2, and L10δ2 using a 5% RAP sample of α-spectrin SH3. (C) The local proximity of those residues is illustrated using the crystal structure (PDB 1U06).[46] Reproduced with permission from ref 26. Copyright 2010 American Chemical Society.

HMQC type sequence. Figure 6B shows the experimental results, focusing on correlations involving Leu10, Ala11, and Met25 in the hydrophobic core of α-spectrin SH3. The ^{13}C resolved ^{1}H(ω_1),^{1}H(ω_3) planes show all expected correlations between Met25ε, Ala11β, Val53γ2, and Leu10δ2. The structure of the protein is represented in Figure 6C. The shortest methyl–methyl proton distances are between 4.5 and 5.6 Å. Similar approaches for determination of proton–proton contacts were proposed, employing perdeuterated and selectively methyl labeled samples.[25,47–49]

^{13}C Backbone and Side Chain Dynamics

Globular proteins are typically tightly packed; however, they can undergo substantial motion on the pico- to microsecond time scale. Often, this motion is linked to function.[50] In the past, we and others have suggested approaches for the quantification of dynamics in the solid state.[24,51–74] For the most part, these experiments rely on ^{15}N, which can be treated as an isolated spin in the protein structure. Even though ^{15}N is a very attractive nucleus to study the dynamic properties of a protein, it comprises at the same time a number of disadvantages: ^{15}N related experiments contain no information on side chain dynamics. In a protein, the amide is typically incorporated into a hydrogen bond either to a carbonyl group within the protein or to a water molecule. This particular property might have an impact on the extracted experimental dynamic parameters. Most importantly, however, the number of possible motional parameters exceeds by far the number of experimental relaxation parameters that can be measured if only ^{15}N is considered, even if experiments at multiple magnetic fields are performed. More observables are needed to allow for an adequate analysis of differential motional models. Obviously, backbone and side chain carbon spins are in principle good candidates. However, care has to be taken to ensure that ^{13}C spins are not directly coupled and, at the same time, that the proton spin system is dilute enough to prevent proton relayed interactions.

To obtain information on incoherent processes, measurement of T_1 times under fast magic angle spinning conditions was proposed,[67] since spin diffusion scales inversely with the MAS frequency.[75] However, spinning only at 60 kHz was still not sufficient to eliminate spin diffusion in uniformly protonated and ^{13}C labeled proteins, as shown for GB1.[67]

In addition to fast spinning, deuteration can be employed, which chemically suppresses spin diffusion.[76] The herein discussed RAP labeling scheme yields uniformly ^{13}C labeled proteins in a deuterated matrix and is, therefore, ideally suited for the quantification of aliphatic ^{13}C T_1 times in a

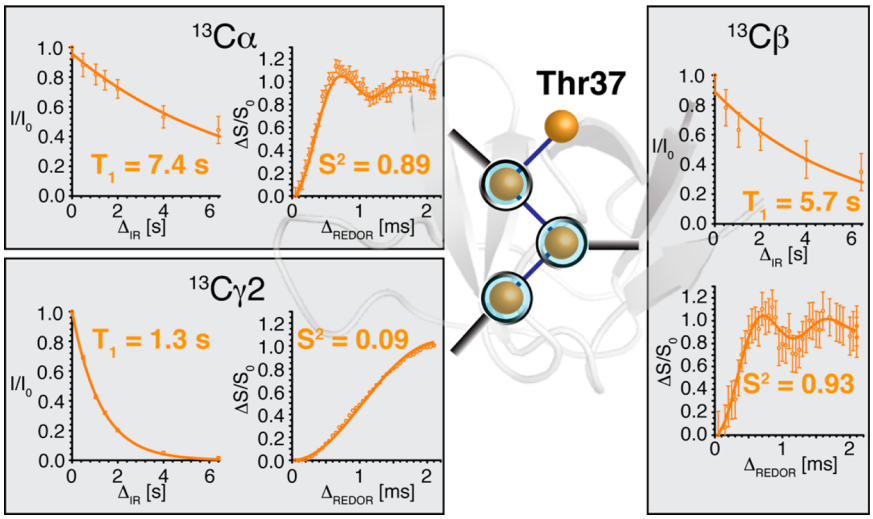

FIGURE 7. Experimental ^{13}C T_1 times and ^{1}H,^{13}C order parameters employing a 15% RAP sample of α-spectrin SH3. T_1 decay, as well as REDOR dephasing curves (using the pulse scheme suggested by Schanda et al.[71]), can be obtained for all carbon sites within the residue, as illustrated here for Thr37. The experiments to determine both dynamical parameters make use of ^{1}H-detection and fast rotation frequencies (≥40 kHz) to yield high sensitivity.

protein and at the same time facilitates the application of ^{1}H detection schemes to improve the experimental sensitivity. In contrast to ^{15}N spectroscopy, which primarily targets the amide backbone, the aliphatic spectrum includes backbone as well as side chain resonances. The excellent dispersion in the aliphatic region and the feasibility to obtain a full assignment (Figure 5) is a prerequisite for any analysis of dynamics.

Figure 7 shows ^{13}C T_1 decay curves for a 15% RAP sample of α-spectrin SH3. The experiments were recorded at a MAS frequency of 50 kHz. The T_1 times for backbone and methyl carbons differ by almost an order of magnitude. The dipolar coupling is a direct probe for sub-microsecond motions because its amplitude is averaged by motions on the respective time scale.[77] In the solid-state, various schemes were introduced to recouple dipolar interactions during MAS.[62,78−81] It turned out that a REDOR type experiment[82] yields the best performance for deuterated proteins in terms of insensitivity to rf miscalibration, rf inhomogeneity, and *I*/*S* spin CSA.[72] The REDOR sequence was applied so far to perdeuterated and selectively ILV methyl labeled samples.[69,71] We show that RAP labeled samples yield at the same time order parameters for all aliphatic sites and ^{13}C T_1 times, using the same sample (Figure 7). A detailed description of the experimental determination of ^{13}C relaxation and order parameters using RAP samples will be given elsewhere.

In the future, analysis of proton and carbon spin dilute protein samples will enable a detailed characterization of backbone and side chain motion with the aim to get insights in the underlying motional models.

This work was supported by the Leibniz-Gemeinschaft, the Helmholtz-Gemeinschaft, the Deutsche Forschungsgemeinschaft (Grants Re1435, SFB1035) and the Bio-NMR project (European Commission's Framework Program 7, project number 261863/ BIO-NMR-00010, BIO-NMR-00070). We are grateful to the Center for Integrated Protein Science Munich (CIPS-M) for financial support and to B. H. Meier (ETH Zürich) for providing measurement time, as well as to Bruker BioSpin, especially to S. Wegner. We acknowledge K. Szekely (ETH Zürich) for technical support and P. Schanda (IBS, Grenoble) for helpful discussions concerning order parameters.

BIOGRAPHICAL INFORMATION

Sam Asami studied biochemistry at the Goethe-Universität in Frankfurt am Main, Germany, and is working toward his Ph.D. since 2009 in the group of B. Reif jointly at the FMP in Berlin and the Technische Universität München. Primarily, he works on method development for solid-state NMR and improvement of labeling strategies to enable dynamical and structural investigations of biomolecules. His research comprises crystalline peptides and proteins, amyloid fibrils, and protein−RNA complexes.

Bernd Reif was born in 1968 in Hof/Saale, Germany. He studied physics and biochemistry at the Universität Bayreuth. In 1998, he received his Ph.D. at the Universität Frankfurt in chemistry where he worked with Christian Griesinger. After a postdoctoral visit in the group of Robert G. Griffin at the Massachusetts Institute of Technology, Cambridge, MA, U.S., he was heading an Emmy-Noether research group of the DFG at the Technische Universität München.

From 2003, Bernd Reif was working as a group leader at the Leibniz-Institut für Molekulare Pharmakologie (FMP) in Berlin. In 2004, he was appointed as a professor at the Charité Universitätsmedizin, Berlin. Since 2010, he is a professor for solid-state NMR at the Technische Universität München. His research focuses on the development of MAS solid-state NMR methods for the characterization of structural and dynamical properties of proteins in the solid state, as well as the application of solution- and solid-state NMR spectroscopy to the study of amyloidogenic peptides and membrane proteins.

FOOTNOTES

*Corresponding author. E-mail: reif@tum.de.
The authors declare no competing financial interest.

REFERENCES

1 Samoson, A.; Tuherm, T.; Past, J.; Reinhold, A.; Anupold, T.; Heinmaa, N. New horizons for magic-angle spinning NMR. *Top. Curr. Chem.* **2005**, *246*, 15–31.

2 Zhou, D. H.; Shah, G.; Cormos, M.; Mullen, C.; Sandoz, D.; Rienstra, C. M. Proton-detected solid-state NMR Spectroscopy of fully protonated proteins at 40 kHz magic-angle spinning. *J. Am. Chem. Soc.* **2007**, *129*, 11791–11801.

3 Marchetti, A.; Jehle, S.; Felletti, M.; Knight, M. J.; Wang, Y.; Xu, Z. Q.; Park, A. Y.; Otting, G.; Lesage, A.; Emsley, L.; Dixon, N. E.; Pintacuda, G. Backbone assignment of fully protonated solid proteins by 1H detection and ultrafast magic-angle-spinning NMR spectroscopy. *Angew. Chem., Int. Ed.* **2012**, *51*, 10756–10759.

4 Chevelkov, V.; van Rossum, B. J.; Castellani, F.; Rehbein, K.; Diehl, A.; Hohwy, M.; Steuernagel, S.; Engelke, F.; Oschkinat, H.; Reif, B. H-1 detection in MAS solid-state NMR spectroscopy of biomacromolecules employing pulsed field gradients for residual solvent suppression. *J. Am. Chem. Soc.* **2003**, *125*, 7788–7789.

5 Morcombe, C. R.; Paulson, E. K.; Gaponenko, V.; Byrd, R. A.; Zilm, K. W. H-1-N-15 correlation spectroscopy of nanocrystalline proteins. *J. Biomol. NMR* **2005**, *31*, 217–230.

6 McDermott, A. E.; Creuzet, F. J.; Kolbert, A. C.; Griffin, R. G. High-resolution magic-angle-spinning NMR spectra of protons in deuterated solids. *J. Magn. Reson.* **1992**, *98*, 408–413.

7 Zheng, L.; Fishbein, K. W.; Griffin, R. G.; Herzfeld, J. Two-dimensional solid-state ^{1}H NMR and proton exchange. *J. Am. Chem. Soc.* **1993**, *115*, 6254–6261.

8 Zorin, V. E.; Brown, S. P.; Hodgkinson, P. Origins of linewidth in 1H magic-angle spinning NMR. *J. Chem. Phys.* **2006**, *125*, No. 144508.

9 Reif, B.; Jaroniec, C. P.; Rienstra, C. M.; Hohwy, M.; Griffin, R. G. ^{1}H-^{1}H MAS correlation spectroscopy and distance measurements in a deuterated peptide. *J. Magn. Reson.* **2001**, *151*, 320–327.

10 Reif, B.; Griffin, R. G. ^{1}H detected ^{1}H,^{15}N correlation spectroscopy in rotating solids. *J. Magn. Reson.* **2003**, *160*, 78–83.

11 Zhou, D. H.; Graesser, D. T.; Franks, W. T.; Rienstra, C. M. Sensitivity and resolution in proton solid-state NMR at intermediate deuteration levels: Quantitative linewidth analysis and applications to correlation spectroscopy. *J. Magn. Reson.* **2006**, *178*, 297–307.

12 Reif, B.; van Rossum, B. J.; Castellani, F.; Rehbein, K.; Diehl, A.; Oschkinat, H. Characterization of ^{1}H ^{1}H distances in a uniformly ^{2}H,^{15}N labeled SH3 domain by MAS solid state NMR spectroscopy. *J. Am. Chem. Soc.* **2003**, *125*, 1488–1489.

13 Paulson, E. K.; Morcombe, C. R.; Gaponenko, V.; Dancheck, B.; Byrd, R. A.; Zilm, K. W. High-sensitivity observation of dipolar exchange and NOEs between exchangeable protons in proteins by 3D solid-state NMR spectroscopy. *J. Am. Chem. Soc.* **2003**, *125*, 14222–14223.

14 Paulson, E. K.; Morcombe, C. R.; Gaponenko, V.; Dancheck, B.; Byrd, R. A.; Zilm, K. W. Sensitive high resolution inverse detection NMR spectroscopy of proteins in the solid state. *J. Am. Chem. Soc.* **2003**, *125*, 15831–15836.

15 Chevelkov, V.; Rehbein, K.; Diehl, A.; Reif, B. Ultra-high resolution in proton solid-state NMR at high levels of deuteration. *Angew. Chem., Int. Ed.* **2006**, *45*, 3878–3881.

16 Akbey, Ü.; Lange, S.; Franks, T. W.; Linser, R.; Diehl, A.; van Rossum, B. J.; Reif, B.; Oschkinat, H. Optimum levels of exchangeable protons in perdeuterated proteins for proton detection in MAS solid-state NMR spectroscopy. *J. Biomol. NMR* **2010**, *46*, 67–73.

17 Lewandowski, J. R.; Dumez, J. N.; Akbey, U.; Lange, S.; Emsley, L.; Oschkinat, H. Enhanced resolution and coherence lifetimes in the solid-state NMR spectroscopy of perdeuterated proteins under ultrafast magic-angle spinning. *J. Phys. Chem. Lett.* **2011**, *2*, 2205–2211.

18 Linser, R.; Dasari, M.; Hiller, M.; Higman, V.; Fink, U.; Lopez del Amo, J.-M.; Handel, L.; Kessler, B.; Schmieder, P.; Oesterhelt, D.; Oschkinat, H.; Reif, B. Proton detected solid-state NMR of fibrillar and membrane proteins. *Angew. Chem., Int. Ed.* **2011**, *50*, 4508–4512.

19 Morris, V. K.; Linser, R.; Wilde, K. L.; Duff, A. P.; Sunde, M.; Kwan, A. H. Solid-state NMR spectroscopy of functional amyloid from a fungal hydrophobin: A well-ordered beta-sheet core amidst structural heterogeneity. *Angew. Chem., Int. Ed.* **2012**, *51*, 12621–12625.

20 Zhou, D. H.; Nieuwkoop, A. J.; Berthold, D. A.; Comellas, G.; Sperling, L. J.; Tang, M.; Shah, G. J.; Brea, E. J.; Lemkau, L. R.; Rienstra, C. M. Solid-state NMR analysis of membrane proteins and protein aggregates by proton detected spectroscopy. *J. Biomol. NMR* **2012**, *54*, 291–305.

21 Ward, M. E.; Shi, L.; Lake, E.; Krishnamurthy, S.; Hutchins, H.; Brown, L. S.; Ladizhansky, V. Proton-detected solid-state NMR reveals intramembrane polar networks in a seven-helical transmembrane protein proteorhodopsin. *J. Am. Chem. Soc.* **2011**, *133*, 17434–17443.

22 Asami, S.; Rakwalska-Bange, M.; Carlomagno, T.; Reif, B. Protein-RNA interfaces probed by (1) H-detected MAS solid-state NMR spectroscopy. *Angew. Chem., Int. Ed.* **2013**, *52*, 2345–2349.

23 Agarwal, V.; Diehl, A.; Skrynnikov, N.; Reif, B. High resolution H-1 detected H-1,C-13 correlation spectra in MAS solid-state NMR using deuterated proteins with selective H-1, H-2 isotopic labeling of methyl groups. *J. Am. Chem. Soc.* **2006**, *128*, 12620–12621.

24 Agarwal, V.; Xue, Y.; Reif, B.; Skrynnikov, N. R. Protein side-chain dynamics as observed by solution- and solid-state NMR spectroscopy: A similarity revealed. *J. Am. Chem. Soc.* **2008**, *130*, 16611–16621.

25 Huber, M.; Hiller, S.; Schanda, P.; Ernst, M.; Bockmann, A.; Verel, R.; Meier, B. H. A proton-detected 4D solid-state NMR experiment for protein structure determination. *ChemPhysChem* **2011**, *12*, 915–918.

26 Asami, S.; Schmieder, P.; Reif, B. High resolution H-1-detected solid-state NMR spectroscopy of protein aliphatic resonances: Access to tertiary structure information. *J. Am. Chem. Soc.* **2010**, *132*, 15133–15135.

27 Shaka, A. J.; Keeler, J.; Frenkiel, T.; Freeman, R. An improved sequence for broad-band decoupling - Waltz-16. *J. Magn. Reson.* **1983**, *52*, 335–338.

28 Agarwal, V.; Reif, B. Residual methyl protonation in perdeuterated proteins for multidimensional correlation experiments in MAS solid-state NMR spectroscopy. *J. Magn. Reson.* **2008**, *194*, 16–24.

29 Asami, S.; Szekely, K.; Schanda, P.; Meier, B. H.; Reif, B. Optimal degree of protonation for 1H detection of aliphatic sites in randomly deuterated proteins as a function of the MAS frequency. *J. Biomol. NMR* **2012**, *54*, 155–168.

30 Asami, S.; Reif, B. Assignment strategies for aliphatic protons in the solid-state in randomly protonated proteins. *J. Biomol. NMR* **2012**, *52*, 31–39.

31 Leppert, J.; Heise, B.; Ohlenschlager, O.; Gorlach, M.; Ramachandran, R. Broadband RFDR with adiabatic inversion pulses. *J. Biomol. NMR* **2003**, *26*, 13–24.

32 Szeverenyi, N. M.; Sullivan, M. J.; Maciel, G. E. Observation of spin exchange by two-dimensional fourier-transform C-13 cross polarization-magic-angle spinning. *J. Magn. Reson.* **1982**, *47*, 462–475.

33 Morcombe, C. R.; Gaponenko, V.; Byrd, R. A.; Zilm, K. W. Diluting abundant spins by isotope edited radio frequency field assisted diffusion. *J. Am. Chem. Soc.* **2004**, *126*, 7196–7197.

34 Takegoshi, K.; Nakamura, S.; Terao, T. C-13-H-1 dipolar-assisted rotational resonance in magic-angle spinning NMR. *Chem. Phys. Lett.* **2001**, *344*, 631–637.

35 Huang, K. Y.; Siemer, A. B.; McDermott, A. E. Homonuclear mixing sequences for perdeuterated proteins. *J. Magn. Reson.* **2011**, *208*, 122–127.

36 Akbey, U.; Oschkinat, H.; van Rossum, B. J. Double-nucleus enhanced recoupling for efficient C-13 MAS NMR correlation spectroscopy of perdeuterated proteins. *J. Am. Chem. Soc.* **2009**, *131*, 17054–17055.

37 Linser, R.; Chevelkov, V.; Diehl, A.; Reif, B. Sensitivity enhancement using paramagnetic relaxation in MAS solid state NMR of perdeuterated proteins. *J. Magn. Reson.* **2007**, *189*, 209–216.

38 Wickramasinghe, N. P.; Parthasarathy, S.; Jones, C. R.; Bhardwaj, C.; Long, F.; Kotecha, M.; Mehboob, S.; Fung, L. W.; Past, J.; Samoson, A.; Ishii, Y. Nanomole-scale protein solid-state NMR by breaking intrinsic 1HT1 boundaries. *Nat Methods* **2009**, *6*, 215–218.

39 Akbey, U.; Camponeschi, F.; van Rossum, B.-J.; Oschkinat, H. Triple resonance cross-polarization for more sensitive (13)C MAS NMR spectroscopy of deuterated proteins. *ChemPhysChem* **2011**, *12*, 2092–2096.

40 Chevelkov, V.; Chen, Z.; Bermel, W.; Reif, B. Resolution enhancement in MAS solid-state NMR by application of 13C homonuclear scalar decoupling during acquisition. *J. Magn. Reson.* **2005**, *172*, 56–62.

41 Wei, D.; Akbey, Ü.; Paaske, B.; Oschkinat, H.; Reif, B.; Bjerring, M.; Nielsen, N. C. Optimal ^{2}H rf pulses and ^{2}H–^{13}C cross-polarization methods for solid-state ^{2}H MAS NMR of perdeuterated proteins. *J. Phys. Chem. Lett.* **2011**, *2*, 1289–1294.

42 Castellani, F.; van Rossum, B.-J.; Diehl, A.; Schubert, M.; Rehbein, K.; Oschkinat, H. Structure of a protein determined by solid-state magic-angle spinning NMR. *Nature* **2002**, *420*, 98–102.

43 Rienstra, C. M.; Hohwy, M.; Mueller, L.; Jaroniec, C. P.; Reif, B.; Griffin, R. G. Determination of multiple torsion-angle constraints in U-^{13} C,^{15} N-labeled peptides: 3D ^{1}H-^{15}N-^{13}C-^{1}H dipolar chemical shift NMR spectroscopy in rotating solids. *J. Am. Chem. Soc.* **2002**, *124*, 11908–11922.

44 Lange, A.; Luca, S.; Baldus, M. Structural constraints from proton-mediated rare-spin correlation spectroscopy in rotating solids. *J. Am. Chem. Soc.* **2002**, *124*, 9704–9705.

45 Loquet, A.; Laage, S.; Gardiennet, C.; Elena, B.; Emsley, L.; Bockmann, A.; Lesage, A. Methyl proton contacts obtained using heteronuclear through-bond transfers in solid-state NMR spectroscopy. *J. Am. Chem. Soc.* **2008**, *130*, 10625–10632.

46 Chevelkov, V.; Faelber, K.; Diehl, A.; Heinemann, U.; Oschkinat, H.; Reif, B. Detection of dynamic water molecules in a microcrystalline sample of the SH3 domain of alpha-spectrin by MAS solid-state NMR. *J. Biomol. NMR* **2005**, *31*, 295–310.

47 Linser, R.; Bardiaux, B.; Higman, V.; Fink, U.; Reif, B. Structure calculation from unambiguous long-range amide and methyl ^{1}H-^{1}H distance restraints for a microcrystalline protein with MAS solid-state NMR spectroscopy. *J. Am. Chem. Soc.* **2011**, *133*, 5905–5912.

48 Knight, M. J.; Webber, A. L.; Pell, A. J.; Guerry, P.; Barbet-Massin, E.; Bertini, I.; Felli, I. C.; Gonnelli, L.; Pierattelli, R.; Emsley, L.; Lesage, A.; Herrmann, T.; Pintacuda, G. Fast resonance assignment and fold determination of human superoxide dismutase by high-resolution proton-detected solid-state MAS NMR spectroscopy. *Angew. Chem., Int. Ed.* **2011**, *50*, 11697–11701.

49 Zhou, D. H.; Shea, J. J.; Nieuwkoop, A. J.; Franks, W. T.; Wylie, B. J.; Mullen, C.; Sandoz, D.; Rienstra, C. M. Solid-rate protein-structure determination with proton-detected triple-resonance 3D magic-angle-spinning NMR spectroscopy. *Angew. Chem., Int. Ed.* **2007**, *46*, 8380–8383.

50 Henzler-Wildman, K. A.; Lei, M.; Thai, V.; Kerns, S. J.; Karplus, M.; Kern, D. A hierarchy of timescales in protein dynamics is linked to enzyme catalysis. *Nature* **2007**, *450*, 913–916.

51 Torchia, D. A.; Szabo, A. Spin-lattice relaxation in solids. *J. Magn. Reson.* **1982**, *49*, 107–121.

52 Reif, B.; Hohwy, M.; Jaroniec, C. P.; Rienstra, C. M.; Griffin, R. G. NH-NH vector correlation in peptides by solid-state NMR. *J. Magn. Reson.* **2000**, *145*, 132–141.

53 Giraud, N.; Blackledge, M.; Goldman, M.; Bockmann, A.; Lesage, A.; Penin, F.; Emsley, L. Quantitative analysis of backbone dynamics in a crystalline protein from nitrogen-15 spin-lattice relaxation. *J. Am. Chem. Soc.* **2005**, *127*, 18190–18201.

54 Hologne, M.; Faelber, K.; Diehl, A.; Reif, B. Characterization of dynamics of perdeuterated proteins by MAS solid-state NMR. *J. Am. Chem. Soc.* **2005**, *127*, 11208–11209.

55 Hologne, M.; Chen, Z. J.; Reif, B. Characterization of dynamic processes using deuterium in uniformly H-2, C-13, N-15 enriched peptides by MAS solid-state NMR. *J. Magn. Reson.* **2006**, *179*, 20–28.

56 Hologne, M.; Chevelkov, V.; Reif, B. Deuterated peptides and proteins in MAS solid-state NMR. *Prog. Nucl. Magn. Reson. Spectrosc.* **2006**, *48*, 211–232.

57 Reif, B.; Xue, Y.; Agarwal, V.; Pavlova, M. S.; Hologne, M.; Diehl, A.; Ryabov, Y. E.; Skrynnikov, N. R. Protein side-chain dynamics observed by solution- and solid-state NMR: Comparative analysis of methyl H-2 relaxation data. *J. Am. Chem. Soc.* **2006**, *128*, 12354–12355.

58 Chevelkov, V.; Diehl, A.; Reif, B. Quantitative measurement of differential N-15-H-alpha/beta T-2 relaxation rates in a perdeuterated protein by MAS solid-state NMR spectroscopy. *Magn. Reson. Chem.* **2007**, *45*, S156–S160.

59 Chevelkov, V.; Zhuravleva, A. V.; Xue, Y.; Reif, B.; Skrynnikov, N. R. Combined analysis of N-15 relaxation data from solid- and solution-state NMR Spectroscopy. *J. Am. Chem. Soc.* **2007**, *129*, 12594–+.

60 Chevelkov, V.; Reif, B. TROSY effects in MAS solid-state NMR. *Concepts Magn. Reson., Part A* **2008**, *32A*, 143–156.

61 Chevelkov, V.; Diehl, A.; Reif, B. Measurement of N-15-T-1 relaxation rates in a perdeuterated protein by magic angle spinning solid-state nuclear magnetic resonance spectroscopy. *J. Chem. Phys.* **2008**, *128*, No. 052316.

62 Chevelkov, V.; Fink, U.; Reif, B. Accurate determination of order parameters from H-1,N-15 dipolar couplings in MAS solid-state NMR experiments. *J. Am. Chem. Soc.* **2009**, *131*, 14018–14022.

63 Chevelkov, V.; Fink, U.; Reif, B. Quantitative analysis of backbone motion in proteins using MAS solid-state NMR spectroscopy. *J. Biomol. NMR* **2009**, *45*, 197–206.

64 Agarwal, V.; Linser, R.; Fink, U.; Faelber, K.; Reif, B. Identification of hydroxyl protons, determination of their exchange dynamics, and characterization of hydrogen bonding in a microcrystallin protein. *J. Am. Chem. Soc.* **2010**, *132*, 3187–3195.

65 Chevelkov, V.; Xue, Y.; Linser, R.; Skrynnikov, N. R.; Reif, B. Comparison of solid-state dipolar couplings and solution relaxation data provides insight into protein backbone dynamics. *J. Am. Chem. Soc.* **2010**, *132*, 5015–5017.

66 Krushelnitsky, A.; Zinkevich, T.; Reichert, D.; Chevelkov, V.; Reif, B. Microsecond time scale mobility in a solid protein as studied by the N-15 R-1 rho site-specific NMR relaxation rates. *J. Am. Chem. Soc.* **2010**, *132*, 11850–11853.

67 Lewandowski, J. R.; Sein, J.; Sass, H. J.; Grzesiek, S.; Blackledge, M.; Emsley, L. Measurement of site-specific 13C spin-lattice relaxation in a crystalline protein. *J. Am. Chem. Soc.* **2010**, *132*, 8252–8254.

68 Lewandowski, J. R.; Sein, J.; Blackledge, M.; Emsley, L. Anisotropic collective motion contributes to nuclear spin relaxation in crystalline proteins. *J. Am. Chem. Soc.* **2010**, *132*, 1246–1248.

69 Schanda, P.; Meier, B. H.; Ernst, M. Quantitative analysis of protein backbone dynamics in microcrystalline ubiquitin by solid-state NMR spectroscopy. *J. Am. Chem. Soc.* **2010**, *132*, 15957–15967.

70 Lewandowski, J. R.; Sass, H. J.; Grzesiek, S.; Blackledge, M.; Emsley, L. Site-specific measurement of slow motions in proteins. *J. Am. Chem. Soc.* **2011**, *133*, 16762–16765.

71 Schanda, P.; Huber, M.; Boisbouvier, J.; Meier, B. H.; Ernst, M. Solid-state NMR measurements of asymmetric dipolar couplings provide insight into protein side-chain motion. *Angew. Chem., Int. Ed.* **2011**, *50*, 11005–11009.

72 Schanda, P.; Meier, B. H.; Ernst, M. Accurate measurement of one-bond H-X heteronuclear dipolar couplings in MAS solid-state NMR. *J. Magn. Reson.* **2011**, *210*, 246–259.

73 Reif, B. Ultra-high resolution in MAS solid-state NMR of perdeuterated proteins: Implications for structure and dynamics. *J. Magn. Reson.* **2012**, *216*, 1–12.

74 Tollinger, M.; Sivertsen, A. C.; Meier, B. H.; Ernst, M.; Schanda, P. Site-resolved measurement of microsecond-to-millisecond conformational-exchange processes in proteins by solid-state NMR spectroscopy. *J. Am. Chem. Soc.* **2012**, *134*, 14800–14807.

75 Kubo, A.; Mcdowell, C. A. Spectral spin diffusion in polycrystalline solids under magic-angle spinning. *J. Chem. Soc., Faraday Trans. I* **1988**, *84*, 3713–3730.

76 Giraud, N.; Blackledge, M.; Bockmann, A.; Emsley, L. The influence of nitrogen-15 proton-driven spin diffusion on the measurement of nitrogen-15 longitudinal relaxation times. *J. Magn. Reson.* **2007**, *184*, 51–61.

77 Gross, J. D.; Warschawski, D. E.; Griffin, R. G. Dipolar recoupling in MAS NMR: A probe for segmental order in lipid bilayers. *J. Am. Chem. Soc.* **1997**, *119*, 796–802.

78 Roberts, J. E.; Harbison, G. S.; Munowitz, M. G.; Herzfeld, J.; Griffin, R. G. Measurement of heteronuclear bond distances in polycrystalline solids by solid-state NMR techniques. *J. Am. Chem. Soc.* **1987**, *109*, 4163–4169.

79 Hohwy, M.; Jaroniec, C. P.; Reif, B.; Rienstra, C. M.; Griffin, R. G. Local structure and relaxation in solid-state NMR: Accurate measurement of amide N−H bond lengths and H−N−H bond angles. *J. Am. Chem. Soc.* **2000**, *122*, 3218–3219.

80 Zhao, X.; Eden, M.; Levitt, M. H. Recoupling of heteronuclear dipolar interactions in solid-state NMR using symmetry-based pulse sequences. *Chem. Phys. Lett.* **2001**, *342*, 353–361.

81 Dvinskikh, S. V.; Zimmermann, H.; Maliniak, A.; Sandstrom, D. Separated local field spectroscopy of columnar and nematic liquid crystals. *J. Magn. Reson.* **2003**, *163*, 46–55.

82 Gullion, T.; Schaefer, J. Rotational-echo double-resonance NMR. *J. Magn. Reson.* **1989**, *81*, 196–200.